THE LANCET
Rheumatology

Supplementary appendix

This appendix formed part of the original submission and has been peer reviewed. We post it as supplied by the authors.

Supplement to: Bressem K, Torgutalp M, Diekhoff T, et al. Prevalence and determinants of sacroiliac joint bone marrow oedema in the general population in Germany: a population-based cross-sectional study. *Lancet Rheumatol* 2026; published online May 6. https://doi.org/10.1016/S2665-9913(26)00071-8.

Appendix

Prevalence and Determinants of Sacroiliac Joint Bone Marrow Edema in the General Population: A Population-Based Cross-Sectional Study

Table of Contents

1 Development of AI Pipeline

1.1 Annotation Process

Three experts in musculoskeletal radiology and rheumatology (DP, TD, NK) independently reviewed all selected cases for the presence of inflammatory changes in the sacroiliac joints, specifically bone marrow edema (BME). The readers simultaneously evaluated PDFS and VIBE images to provide contextual interpretation of signal alterations, characterizing both the presence and anatomical distribution of inflammatory changes. All readers were blinded to demographic and clinical information to prevent bias.

We established a consensus reference standard, defining BME positivity as the presence of hyperintense signal on PDFS sequences in the subchondral bone marrow of the sacroiliac joints, confirmed by at least two of three readers. Of the 998 expert-read cases, 288 (28.9%) demonstrated BME according to this consensus.

All consensus-positive BME cases underwent detailed volumetric annotation with pixel-wise segmentation of edematous regions. Expert segmentations were performed using 3D Slicer (version 4.11) with MONAI Label integration[1] in a multi-stage approach. Initial segmentations were conducted by a resident radiologist (LX) with assistance from a preliminary deep learning model to expedite the annotation process. All segmentations underwent subsequent independent review by a senior radiologist.

Concurrently, anatomical segmentation masks were manually generated for a subset of cases by a board certified radiologist (JLV) and a radiology resident (LX) on both VIBE (n=148) and PDFS (n=50). For VIBE images, the annotated classes included right ilium, sacrum, left ilium, right proximal femur, left proximal femur, and the fifth lumbar vertebra; PDFS images were segmented into pelvis and spine.

1.2 Image Preprocessing and Registration Pipeline

We implemented a comprehensive preprocessing workflow to standardize image data and ensure anatomical correspondence between imaging sequences. All DICOM (Digital Imaging and Communications in Medicine) series were converted to Nearly Raw Raster Data (NRRD) format using SimpleITK (version 2.1).[2] Both PDFS and VIBE volumes underwent isotropic resampling to 1 mm^3 voxel spacing using B-spline interpolation to establish uniform spatial resolution across all cases.

For multimodal image alignment, we employed a registration framework with PDFS images serving as the reference volume. VIBE images were registered to their corresponding PDFS counterparts using a two-stage approach: (1) initial rigid registration based on mutual information, followed by (2) refined deformable registration guided by anatomical segmentation masks.

Following registration, we generated a precise sacroiliac joint mask through morphological operations on the segmentation masks. Specifically, the VIBE-derived masks of the sacrum and ilium underwent morphological dilation (3 mm spherical structuring element, iterated 30 times for sacral and 10 times for iliac masks), creating an intersection region that accurately delineated the sacroiliac joint space and adjacent subchondral bone. This defined region served as the focused field of view for subsequent BME analysis.

Both registered VIBE and PDFS volumes were then cropped to the minimal bounding box containing the sacroiliac joint region with 10 mm additional margin, reducing computational overhead and focusing the analysis on the anatomical region most relevant for BME assessment.

1.3 Deep Learning Framework for BME Detection and Segmentation

We developed a dual-component deep learning framework for anatomical structure segmentation and BME lesion detection and quantification. The pipeline is visualized in Supplementary Figure 1.

1.3.1 Anatomical Segmentation Models

Two dedicated models were implemented for anatomical segmentation using the MONAI framework for Python (version 1.3.2).[3] Both models utilized the MONAI bundle system for modular configuration and shared as common architectural foundation a 3D U-Net with four residual encoding blocks (channel depths of 64, 128, 256, and 512), kernel size of 3×3×3, stride of 2, and random weight initialization. All models were trained from scratch without transfer learning.

The VIBE-based segmentation model was optimized to identify six distinct anatomical structures (right ilium, sacrum, left ilium, right femur, left femur, fifth lumbar vertebra) with a combination of Dice and cross-entropy loss functions (weighting 0.5:0.5) and AdamW optimizer (adaptive learning rate following a one-cycle policy with 1e-4 base, weight decay: 1e-2). Training proceeded for 100 epochs with checkpointing based on validation performance.

The PDFS-based model was developed for binary segmentation of pelvic structures, trained using the same loss functions and optimization strategy. Although PDFS sequences provide excellent soft tissue contrast, delineation of fine anatomical boundaries such as the joint space can be challenging; therefore, we incorporated both modalities into our pipeline to leverage their complementary strengths.

1.3.2 BME Segmentation Model

For BME detection and segmentation, we implemented a 3D U-Net with identical architecture to the anatomical segmentation models but trained exclusively on PDFS sequences, which depict BME as a hyperintense signal. The model was trained using 5-fold cross-validation with 230/58 samples in the training/validation split for each fold. Training proceeded for 500 epochs, using a combination of Dice and cross-entropy loss functions (weighting ratio 0.5:0.5) to address class imbalance between BME and background tissue.

Post-processing incorporated structure-aware constraints by applying the sacroiliac joint masks generated from anatomical segmentations to restrict BME predictions to clinically relevant regions. Furthermore, morphological opening operations were applied to remove very small regions, minimizing false positive segmentations.

The validated segmentation pipeline was subsequently applied to the remaining 10,165 participants with available imaging data. BME volume was quantified by counting voxels classified as edema (each voxel representing 1 mm^3), providing a continuous metric of BME burden (hereafter referred to as "numerical BME"). To classify the presence of BME on the patient level (hereafter referred to as "balanced BME"), we used a volume threshold of 0.91 cm^3, calibrated to match the observed BME prevalence in the expert-read cohort.

Table 1: Segmentation Performance for Bone Marrow Edema (5-fold cross-validation)

Fold	**Mean Dice (95% CI)**	**Mean Hausdorff (95% CI)**
1	0.78 [0.74–0.81]	34.9 [28.5–42.8]
2	0.79 [0.76–0.82]	28.3 [22.0–36.0]
3	0.82 [0.79–0.84]	28.4 [21.2–36.9]
4	0.79 [0.76–0.82]	33.6 [24.9–42.7]
5	0.81 [0.79–0.83]	33.2 [25.3–41.6]
Average	**0.79 [0.78–0.81]**	**31.7 [28.3–35.3]**

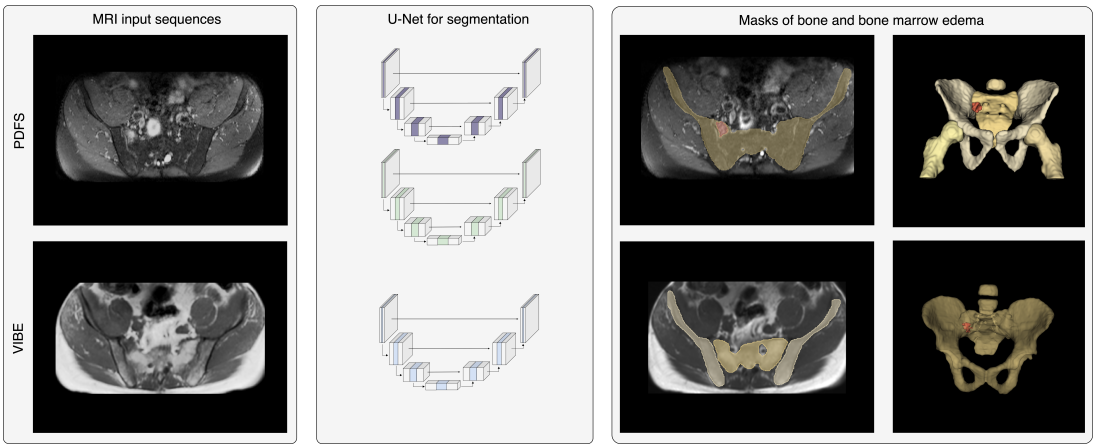

Figure 1: The pipeline ingests pelvic MRI using fat-suppressed proton-density (PDFS) and T1-weighted Dixon VIBE sequences, processes slices with a U-Net, and outputs voxel-wise masks of pelvic bone and bone marrow edema. Example results show overlayed segmentations on axial images and corresponding 3D renderings of bone with localized edema.

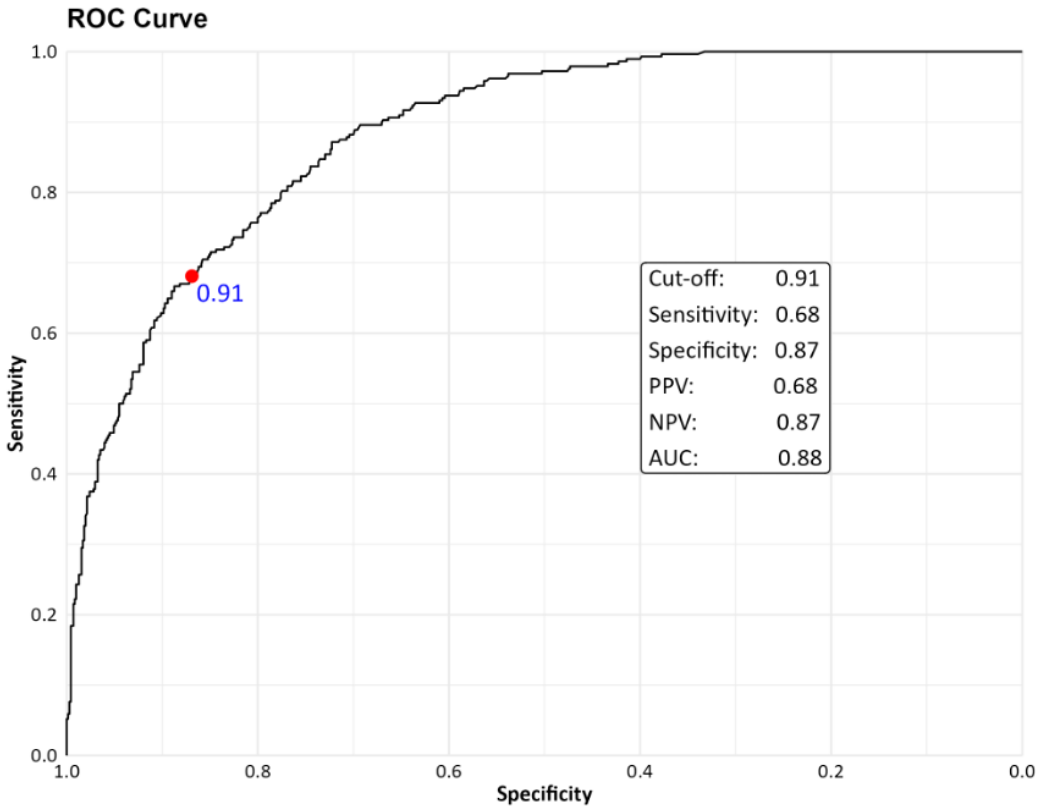

Figure 2: Receiver Operating Characteristic (ROC) Curve for Model-Based Classification of BME Using Expert-Read Reference Standard.

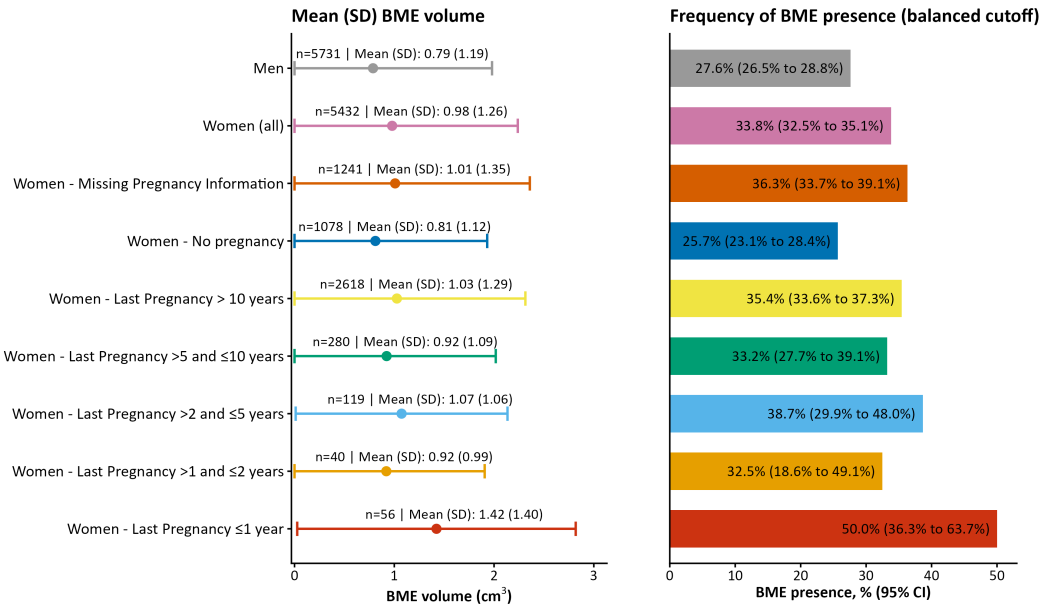

Figure 3: Sacroiliac joint BME volume and BME prevalence (balanced cutoff) by time since last pregnancy in women, with male reference group.

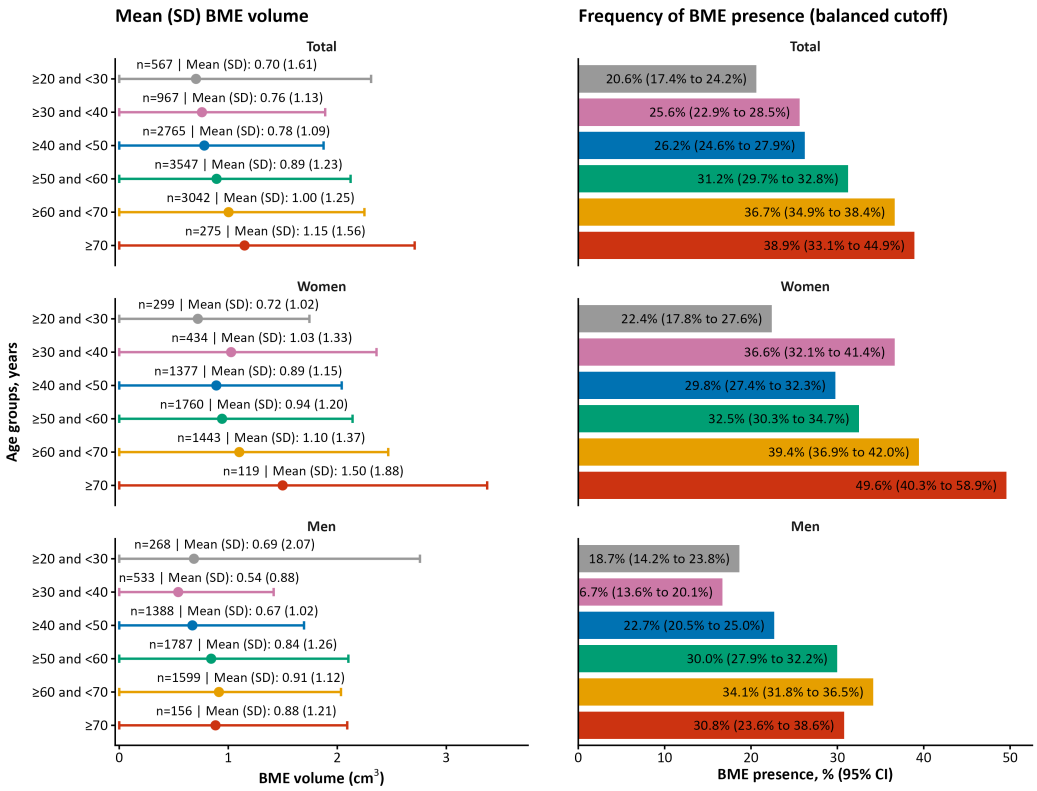

Figure 4: Sacroiliac joint BME volume and BME prevalence (balanced cutoff) across age groups, overall and sex-stratified.

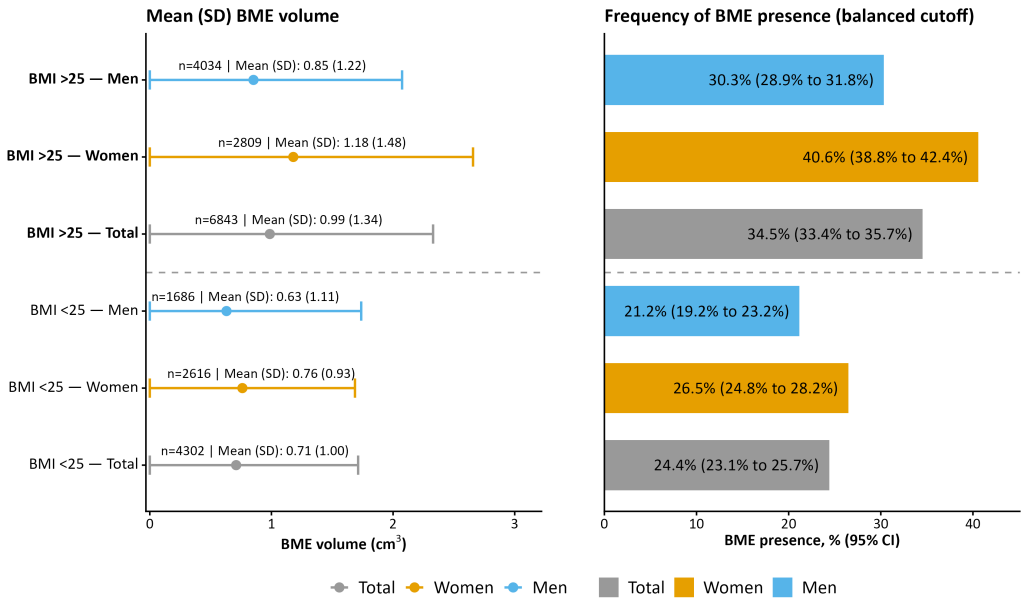

Figure 5: Sacroiliac joint BME volume and BME prevalence (balanced cutoff) by BMI category ($\geq$25 vs <25 kg/m^2), overall and sex-stratified.

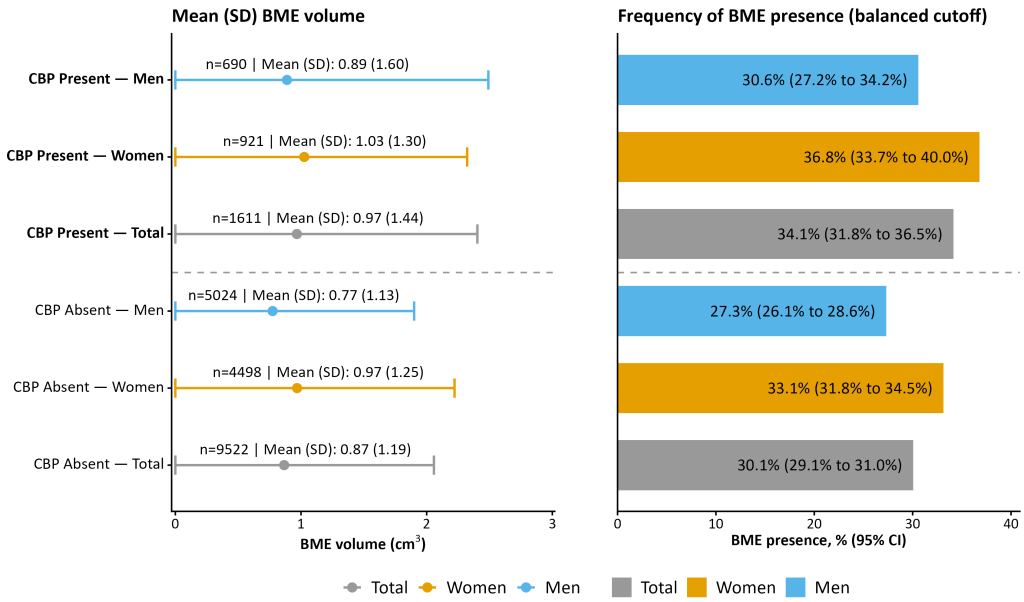

Figure 6: Sacroiliac joint BME volume and BME prevalence (balanced cutoff) by chronic back pain status, overall and sex-stratified.

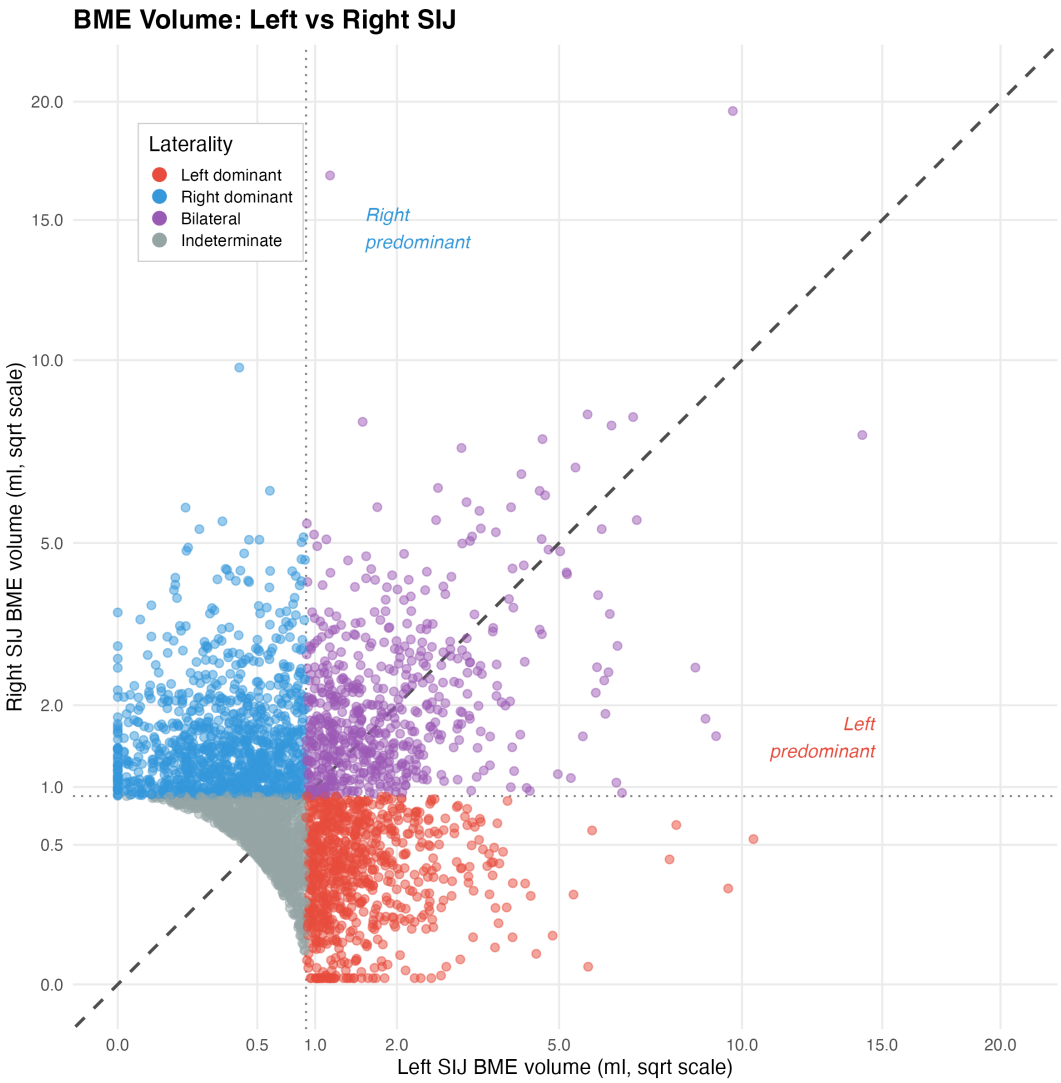

Figure 7: Left versus right SIJ BME volume for participants with detectable BME in the AI anlyzed cohort. Diagonal line indicates symmetric involvement, dotted lines mark the 0.91 ml threshold defining clinically relevant BME. Colors indicate laterality: left dominant (red), right dominant (blue), bilateral (purple), and indeterminate (gray). Axes are square-root transformed. Unilateral involvement predominated over bilateral.

2 Anatomical Segmentation Performance

The automated segmentation model for pelvic structures in PDFS images demonstrated robust performance, achieving a mean Dice similarity coefficient of 0.86 (95% CI: 0.85–0.86) and a mean Hausdorff distance (95th percentile) of 3.6 mm (95% CI: 3.3–4.0). Cross-validation analysis revealed consistent performance across all five folds, with no statistically significant variation for either Dice coefficient (p=0.381) or Hausdorff distance (p=0.159). Mean Dice scores ranged from 0.851 to 0.861 across folds.

The fifth lumbar vertebra was most challenging for the model, yielding the lowest Dice coefficient of 0.66 (95% CI: 0.61–0.70). This likely reflects the complex morphology and partial volume effects at the superior boundary of the imaging field.

Hausdorff distances showed a similar pattern, with the most accurate alignment observed in the sacrum (4.0 mm, 95% CI: 2.7–5.7 mm) and proximal femora (left: 5.5 mm, 95% CI: 2.7–9.2 mm; right: 5.3 mm, 95% CI: 2.6–8.6 mm), while the pelvic bones demonstrated slightly higher distances (left: 7.8 mm, 95% CI: 4.9–11.4 mm; right: 7.1 mm, 95% CI: 4.6–10.3 mm). Cross-validation ANOVA confirmed no statistically significant inter-fold differences (p>0.05) for any of the six anatomical structures.

Table 2: Segmentation Performance: Whole Pelvis in PDFS (Dice Coefficient)

Fold	**Mean Dice (95% CI)**	**Mean Hausdorff 95 (95% CI)**
1	0.86 [0.85–0.87]	3.1 [2.8–3.4]
2	0.86 [0.85–0.87]	3.0 [2.8–3.3]
3	0.85 [0.84–0.86]	4.3 [3.4–5.4]
4	0.86 [0.85–0.87]	3.6 [3.0–4.4]
5	0.86 [0.85–0.86]	4.1 [3.0–5.7]
Average	**0.86 [0.85–0.86]**	**3.6 [3.3–4.0]**

Table 3: Segmentation Performance: Pelvis in VIBE

Fold	Left Pelvis	Right Pelvis	Left Prox Femur	Right Prox Femur	Sacrum	L5
Dice Coefficient						
1	0.81 [0.76–0.86]	0.83 [0.79–0.86]	0.87 [0.82–0.90]	0.81 [0.77–0.85]	0.82 [0.78–0.85]	0.63 [0.58–0.68]
2	0.85 [0.82–0.87]	0.86 [0.84–0.88]	0.86 [0.80–0.90]	0.90 [0.86–0.92]	0.83 [0.80–0.86]	0.72 [0.67–0.77]
3	0.83 [0.78–0.86]	0.85 [0.82–0.88]	0.87 [0.81–0.90]	0.84 [0.79–0.87]	0.83 [0.79–0.86]	0.65 [0.58–0.71]
4	0.84 [0.80–0.88]	0.84 [0.79–0.88]	0.87 [0.82–0.90]	0.85 [0.80–0.88]	0.81 [0.78–0.85]	0.69 [0.63–0.74]
5	0.87 [0.84–0.88]	0.86 [0.83–0.88]	0.91 [0.89–0.93]	0.91 [0.89–0.93]	0.83 [0.79–0.86]	0.57 [0.51–0.62]
Mean	**0.84 [0.82–0.85]**	**0.85 [0.83–0.86]**	**0.86 [0.85–0.89]**	**0.86 [0.83–0.88]**	**0.82 [0.82–0.83]**	**0.66 [0.61–0.70]**
Hausdorff Distance (mm)						
1	10.8 [5.0–20.0]	15.1 [7.0–29.7]	2.9 [1.0–6.0]	6.4 [2.0–18.0]	5.1 [2.0–9.1]	6.0 [2.0–11.2]
2	8.9 [3.0–15.0]	4.7 [2.0–11.3]	3.5 [1.0–5.4]	1.5 [1.0–1.7]	2.3 [1.0–2.0]	2.9 [1.5–4.0]
3	9.0 [4.0–28.0]	5.8 [2.0–15.2]	8.8 [3.0–28.7]	11.6 [4.0–31.1]	2.2 [1.0–1.6]	6.6 [2.0–15.2]
4	8.0 [3.0–20.5]	7.3 [2.0–17.6]	10.9 [4.0–34.0]	6.0 [2.0–22.7]	8.2 [2.0–19.4]	4.1 [2.0–4.0]
5	2.3 [1.0–3.7]	2.6 [1.0–6.5]	1.1 [0.3–2.0]	1.1 [0.3–2.0]	2.0 [1.2–3.2]	4.6 [2.0–6.4]
Mean	**7.8 [4.9–11.4]**	**7.1 [4.6–10.3]**	**5.5 [2.7–9.2]**	**5.3 [2.6–8.6]**	**4.0 [2.7–5.7]**	**4.8 [3.5–6.4]**

Table 4: Demographic and clinical characteristics by sex, stratified by expert reader status

	Expert-read subjects		**AI-analyzed subjects**	
Variable	**Women (N=470)**	**Men (N=528)**	**Women (N=4,962)**	**Men (N=5,203)**
Age, years	51.9 ± 11.8	51.9 ± 11.3	51.7 ± 11.3	52.1 ± 11.5
Body mass index, kg/m^2	26.4 ± 5.4	27.4 ± 4.3	26.2 ± 5.2	27.4 ± 4.1
Smoking status				
Current	77 (17.2)	121 (23.9)	892 (18.7)	1,024 (20.3)
Former	121 (27.0)	183 (36.1)	1,355 (28.4)	1,885 (37.4)
Never	250 (55.8)	203 (40.0)	2,521 (52.9)	2,130 (42.3)
Sufficient physical activity (WHO)	395 (84.0)	446 (84.5)	4,229 (85.2)	4,474 (86.0)
Occupational physical activity	234 (49.8)	241 (45.6)	2,213 (44.6)	2,405 (46.2)
Transportation physical activity	317 (67.4)	361 (68.4)	3,359 (67.7)	3,447 (66.3)
Recreational physical activity	352 (74.9)	389 (73.7)	3,717 (74.9)	3,835 (73.7)
Intensive physical activity	278 (59.1)	335 (63.4)	2,767 (55.8)	3,368 (64.7)
Family status, married	294 (62.6)	377 (71.4)	3,116 (62.8)	3,617 (69.5)
University or above education	192 (45.6)	298 (61.2)	2,270 (50.5)	2,923 (61.7)
Socioeconomic status (ISEI-08)	47.2 ± 15.3	51.0 ± 16.1	47.3 ± 14.7	50.9 ± 15.7
History of psoriasis	34 (7.2)	29 (5.6)	290 (5.9)	332 (6.4)
History of IBD	5 (1.1)	7 (1.3)	66 (1.3)	50 (1.0)
Ever CBP	114 (24.3)	124 (23.6)	1,295 (26.2)	1,096 (21.1)
CBP in the last 12 months	75 (16.0)	70 (13.3)	846 (17.1)	620 (12.0)
Known axSpA diagnosis	0 (0.0)	4 (0.8)	25 (0.5)	38 (0.7)
CRP levels, mg/L	2.1 ± 3.2	2.0 ± 3.7	2.4 ± 3.3	2.0 ± 4.4
Elevated CRP (>5 mg/L)	17 (8.4)	17 (7.4)	266 (11.3)	160 (7.0)
Pregnancy ever	341 (76.8)	–	3,783 (79.5)	–
Number of pregnancies	1.9 ± 1.5	–	1.9 ± 1.5	–
Live birth ever	322 (75.6)	–	3,560 (78.1)	–
Number of live births	1.5 ± 1.2	–	1.5 ± 1.1	–
BME volume, cm^3	0.9 ± 1.2	0.9 ± 2.0	1.0 ± 1.3	0.8 ± 1.1
BME Presence (Balanced Cutoff)	152 (32.3)	137 (25.9)	1,684 (33.9)	1,447 (27.8)

Variables are presented as mean ± SD or n (%).
AI = Artificial Intelligence; BME = Bone Marrow Edema; CBP = Chronic Back Pain; CRP = C-reactive protein; IBD = Inflammatory Bowel Disease; WHO = World Health Organization.

Table 5: Multivariable regression models including sex–predictor interaction terms assessing differences in associations between demographic and clinical factors and bone marrow edema outcomes

	Expert-read BME presence		**AI-analyzed BME Presence**		**AI-analyzed BME volume**	
Term	**OR (95% CI)**	**P interaction**	**OR (95% CI)**	**P interaction**	**Beta (95% CI)**	**P interaction**
Female sex (vs male)*	2.70 (0.87, 8.45)	–	2.68 (1.90, 3.80)	–	0.45 (0.28, 0.62)	–
Age, per 10-year increase	1.31 (1.09, 1.59)	0.487	1.25 (1.18, 1.32)	0.001	0.09 (0.07, 0.12)	0.019
BMI, >25 vs <25	1.41 (0.88, 2.30)	0.864	1.45 (1.26, 1.68)	0.025	0.18 (0.11, 0.25)	<0.001
Occupational PA (yes vs no)	1.41 (0.93, 2.14)	0.543	1.34 (1.18, 1.53)	0.092	0.13 (0.06, 0.19)	0.254
Intensive PA (yes vs no)	1.06 (0.69, 1.65)	0.569	1.24 (1.08, 1.42)	0.003	0.13 (0.06, 0.20)	<0.001

*Main effect of sex; interaction p-values test whether the association differs between men and women.

BME = Bone Marrow Edema; BMI = Body Mass Index; CI = Confidence Interval; OR = Odds Ratio; PA = Physical Activity.

Table 6: Multivariable regression analyses stratified by chronic back pain status

	Expert BME presence		**AI BME Presence**		**Expert BME volume**		**AI BME volume**	
Term*	**CBP Absent** OR (95% CI)	**CBP Present** OR (95% CI)	**CBP Absent** OR (95% CI)	**CBP Present** OR (95% CI)	**CBP Absent** Beta (95% CI)	**CBP Present** Beta (95% CI)	**CBP Absent** Beta (95% CI)	**CBP Present** Beta (95% CI)
Female sex (vs male)	1.53 (1.14–2.06)	0.97 (0.47–2.01)	1.31 (1.20–1.44)	1.35 (1.09–1.69)	0.16 (–0.03–0.35)	–0.41 (–1.29–0.47)	0.20 (0.15–0.25)	0.20 (0.07–0.33)
Age, per 10-year	1.34 (1.18–1.54)	0.92 (0.63–1.32)	1.21 (1.17–1.26)	1.19 (1.06–1.33)	0.07 (–0.01–0.15)	–0.42 (–0.86–0.02)	0.09 (0.07–0.11)	0.08 (0.01–0.14)
BMI, >25 vs <25	1.33 (0.94–1.87)	1.62 (0.68–4.05)	1.59 (1.43–1.76)	1.86 (1.44–2.42)	0.36 (0.16–0.57)	0.16 (–0.86–1.17)	0.27 (0.22–0.33)	0.35 (0.21–0.50)
Occupational PA (yes vs no)	1.13 (0.82–1.54)	4.57 (1.70–13.80)	1.24 (1.13–1.37)	1.30 (1.02–1.66)	0.18 (–0.01–0.37)	0.55 (–0.53–1.63)	0.11 (0.06–0.16)	0.12 (–0.02–0.25)
Intensive PA (yes vs no)	0.97 (0.71–1.34)	0.61 (0.22–1.64)	1.06 (0.96–1.17)	1.10 (0.86–1.41)	0.13 (–0.07–0.32)	–0.74 (–1.84–0.36)	0.05 (–0.00–0.10)	–0.05 (–0.19–0.09)

*Models adjusted for age, sex, and BMI as appropriate.

BME = Bone Marrow Edema; BMI = Body Mass Index; CBP = Chronic Back Pain; PA = Physical Activity.

Table 7: Diagnostic summary for linear regression models of BME volume (by subgroup and dataset)

Group	Dataset	Exposure	N	BP p	Corr(|resid|,fit)	|Std resid|>3	Max |Std resid|	Max Cook's D
All	AI-analyzed	Age, per 10-year	10,165	0.014	0.078	198 (1.9%)	14.6	0.0241
All	AI-analyzed	BMI, >25 vs <25	9,639	<0.001	0.174	182 (1.9%)	14.6	0.0199
All	AI-analyzed	Female sex	10,165	0.003	0.058	198 (1.9%)	14.6	0.0205
All	AI-analyzed	Intensive PA	10,150	<0.001	0.169	195 (1.9%)	14.8	0.0188
All	AI-analyzed	Occupational PA	10,150	<0.001	0.169	195 (1.9%)	14.8	0.0188
All	Expert-read	Age, per 10-year	998	0.082	−0.004	15 (1.5%)	17.4	0.9810
All	Expert-read	BMI, >25 vs <25	939	0.306	0.137	13 (1.4%)	17.4	0.5770
All	Expert-read	Female sex	998	0.199	−0.037	16 (1.6%)	17.3	0.2840
All	Expert-read	Intensive PA	995	0.336	0.120	15 (1.5%)	17.6	0.5720
All	Expert-read	Occupational PA	995	0.336	0.120	15 (1.5%)	17.6	0.5720
Females	AI-analyzed	Age, per 10-year	4,962	0.028	0.067	95 (1.9%)	11.3	0.0415
Females	AI-analyzed	BMI, >25 vs <25	4,498	<0.001	0.200	83 (1.8%)	11.2	0.0306
Females	AI-analyzed	Intensive PA	4,751	<0.001	0.201	88 (1.9%)	11.3	0.0352
Females	AI-analyzed	Occupational PA	4,751	<0.001	0.201	88 (1.9%)	11.3	0.0352
Females	AI-analyzed	Pregnancy ever	4,758	0.119	0.078	89 (1.9%)	11.3	0.0394
Females	AI-analyzed	Pregnancy 12 mo	4,758	0.142	0.080	92 (1.9%)	11.4	0.0867
Females	Expert-read	Age, per 10-year	470	0.301	0.137	11 (2.3%)	6.4	0.2730
Females	Expert-read	BMI, >25 vs <25	417	0.007	0.316	10 (2.4%)	6.5	0.0858
Females	Expert-read	Intensive PA	444	0.015	0.319	11 (2.5%)	6.5	0.2060
Females	Expert-read	Occupational PA	444	0.015	0.319	11 (2.5%)	6.5	0.2060
Females	Expert-read	Pregnancy ever	444	0.712	0.113	11 (2.5%)	6.5	0.2270
Males	AI-analyzed	Age, per 10-year	5,203	0.158	0.098	99 (1.9%)	16.0	0.0578
Males	AI-analyzed	BMI, >25 vs <25	4,947	0.003	0.158	94 (1.9%)	15.9	0.0439
Males	AI-analyzed	Intensive PA	5,195	0.017	0.157	99 (1.9%)	16.2	0.0432
Males	AI-analyzed	Occupational PA	5,195	0.017	0.157	99 (1.9%)	16.2	0.0432
Males	Expert-read	Age, per 10-year	528	0.053	0.079	5 (0.9%)	14.5	1.3500
Males	Expert-read	BMI, >25 vs <25	498	0.223	0.156	5 (1.0%)	14.3	0.8280
Males	Expert-read	Intensive PA	525	0.300	0.094	5 (1.0%)	14.6	0.8910
Males	Expert-read	Occupational PA	525	0.300	0.094	5 (1.0%)	14.6	0.8910

BP = Breusch-Pagan test for heteroscedasticity; PA = Physical Activity.

Table 8: Primary estimates and sensitivity analyses (robust standard errors and age functional-form) for linear regression models of BME volume

Group	Dataset	Exposure	Primary Beta (95% CI)	Robust-SE Beta (95% CI)	Age sensitivity Beta (95% CI)
All	AI-analyzed	Female sex (vs male)	0.20 (0.16 to 0.25)	0.20 (0.16 to 0.25)	0.20 (0.16 to 0.25)
All	AI-analyzed	Age, per 10-year	0.09 (0.07 to 0.11)	0.09 (0.07 to 0.11)	–
All	AI-analyzed	BMI, >25 vs <25	0.29 (0.23 to 0.34)	0.29 (0.24 to 0.33)	0.29 (0.24 to 0.34)
All	AI-analyzed	Occupational PA	0.10 (0.06 to 0.15)	0.10 (0.06 to 0.15)	0.10 (0.05 to 0.15)
All	AI-analyzed	Intensive PA	0.03 (–0.01 to 0.08)	0.03 (–0.01 to 0.08)	0.04 (–0.01 to 0.08)
All	Expert-read	Female sex (vs male)	0.09 (–0.12 to 0.29)	0.09 (–0.11 to 0.28)	0.09 (–0.12 to 0.29)
All	Expert-read	Age, per 10-year	0.03 (–0.05 to 0.12)	0.03 (–0.10 to 0.16)	–
All	Expert-read	BMI, >25 vs <25	0.31 (0.08 to 0.54)	0.31 (0.10 to 0.52)	0.34 (0.11 to 0.57)
All	Expert-read	Occupational PA	0.21 (–0.00 to 0.43)	0.21 (0.04 to 0.39)	0.20 (–0.01 to 0.42)
All	Expert-read	Intensive PA	0.02 (–0.20 to 0.24)	0.02 (–0.22 to 0.26)	0.01 (–0.21 to 0.23)
Females	AI-analyzed	Age, per 10-year	0.08 (0.05 to 0.11)	0.08 (0.05 to 0.11)	–
Females	AI-analyzed	BMI, >25 vs <25	0.40 (0.33 to 0.48)	0.40 (0.33 to 0.48)	0.40 (0.33 to 0.48)
Females	AI-analyzed	Occupational PA	0.07 (0.00 to 0.15)	0.07 (–0.00 to 0.15)	0.07 (–0.01 to 0.14)
Females	AI-analyzed	Intensive PA	–0.05 (–0.12 to 0.02)	–0.05 (–0.12 to 0.03)	–0.05 (–0.12 to 0.02)
Females	AI-analyzed	Pregnancy ever	0.15 (0.06 to 0.25)	0.15 (0.06 to 0.24)	0.17 (0.07 to 0.26)
Females	AI-analyzed	Pregnancy 12 mo	0.65 (0.31 to 1.00)	0.65 (0.27 to 1.04)	0.58 (0.23 to 0.92)
Females	Expert-read	Age, per 10-year	0.09 (–0.00 to 0.18)	0.09 (–0.02 to 0.20)	–
Females	Expert-read	BMI, >25 vs <25	0.41 (0.19 to 0.63)	0.41 (0.20 to 0.63)	0.47 (0.25 to 0.69)
Females	Expert-read	Occupational PA	0.35 (0.12 to 0.57)	0.35 (0.12 to 0.57)	0.31 (0.08 to 0.53)
Females	Expert-read	Intensive PA	0.09 (–0.14 to 0.32)	0.09 (–0.14 to 0.32)	0.10 (–0.13 to 0.32)
Females	Expert-read	Pregnancy ever	0.03 (–0.25 to 0.31)	0.03 (–0.23 to 0.28)	0.14 (–0.16 to 0.43)
Males	AI-analyzed	Age, per 10-year	0.11 (0.08 to 0.13)	0.11 (0.08 to 0.13)	–
Males	AI-analyzed	BMI, >25 vs <25	0.17 (0.10 to 0.23)	0.17 (0.11 to 0.23)	0.17 (0.10 to 0.24)
Males	AI-analyzed	Occupational PA	0.13 (0.06 to 0.19)	0.13 (0.07 to 0.18)	0.12 (0.06 to 0.19)
Males	AI-analyzed	Intensive PA	0.13 (0.07 to 0.19)	0.13 (0.07 to 0.19)	0.13 (0.06 to 0.19)
Males	Expert-read	Age, per 10-year	–0.02 (–0.17 to 0.12)	–0.02 (–0.26 to 0.21)	–
Males	Expert-read	BMI, >25 vs <25	0.19 (–0.22 to 0.59)	0.19 (–0.16 to 0.53)	0.33 (–0.08 to 0.73)
Males	Expert-read	Occupational PA	0.16 (–0.19 to 0.52)	0.16 (–0.10 to 0.43)	0.16 (–0.19 to 0.52)
Males	Expert-read	Intensive PA	–0.04 (–0.41 to 0.32)	–0.04 (–0.49 to 0.41)	–0.05 (–0.42 to 0.31)

BME = Bone Marrow Edema; BMI = Body Mass Index; CI = Confidence Interval; PA = Physical Activity; SE = Standard Error.

Table 9: Laterality characteristics of sacroiliac bone marrow edema, stratified by sex

	Expert-read		**AI-analyzed**	
	Women (n=470)	**Men** (n=528)	**Women** (n=4,962)	**Men** (n=5,203)
Volume per side, ml, mean ± SD				
Left SIJ	0.45 ± 0.76	0.38 ± 1.03	0.46 ± 0.71	0.36 ± 0.59
Right SIJ	0.49 ± 0.68	0.48 ± 1.16	0.52 ± 0.76	0.42 ± 0.70
BME laterality pattern, n (%)				
Left SIJ only	35 (7.4)	31 (5.9)	367 (7.4)	334 (6.4)
Right SIJ only	43 (9.1)	46 (8.7)	495 (10.0)	445 (8.6)
Bilateral	27 (5.7)	23 (4.4)	326 (6.6)	237 (4.6)
Indeterminate	46 (9.8)	37 (7.0)	493 (9.9)	426 (8.2)
No BME	318 (67.7)	391 (74.1)	3,279 (66.1)	3,756 (72.2)

BME = Bone Marrow Edema; SIJ = Sacroiliac Joint.

Table 10: STROBE Statement—Checklist of items that should be included in reports of cross-sectional studies

Item No	Recommendation	Reported on page/section
Title and Abstract		
1a	Indicate the study's design with a commonly used term in the title or the abstract	Title; Abstract
1b	Provide in the abstract an informative and balanced summary of what was done and what was found	Abstract
Introduction		
2	Explain the scientific background and rationale for the investigation being reported	Introduction, paragraphs 1–4
3	State specific objectives, including any prespecified hypotheses	Introduction, final paragraph; Abstract (Background)
Methods		
4	Present key elements of study design early in the paper	Methods, Study Design and Participants, paragraph 1
5	Describe the setting, locations, and relevant dates, including periods of recruitment, exposure, follow-up, and data collection	Methods, Study Design and Participants; Methods, Procedures
6	Give the eligibility criteria, and the sources and methods of selection of participants	Methods, Study Design and Participants; Figure 1
7	Clearly define all outcomes, exposures, predictors, potential confounders, and effect modifiers. Give diagnostic criteria, if applicable	Methods, Outcomes; Methods, Study Design and Participants
8	For each variable of interest, give sources of data and details of methods of assessment (measurement). Describe comparability of assessment methods if there is more than one group	Methods, Procedures; Methods, Outcomes; Supplement 1
9	Describe any efforts to address potential sources of bias	Methods, Procedures (blinding of readers); Methods, Statistical Analysis
10	Explain how the study size was arrived at	Methods, Study Design and Participants; Figure 1
11	Explain how quantitative variables were handled in the analyses. If applicable, describe which groupings were chosen and why	Methods, Statistical Analysis; Methods, Study Design and Participants
12a	Describe all statistical methods, including those used to control for confounding	Methods, Statistical Analysis

Continued on next page

Table S10 continued from previous page

Item No	Recommendation	Reported on page/section
12b	Describe any methods used to examine subgroups and interactions	Methods, Statistical Analysis (sex-stratified analyses, interaction terms)
12c	Explain how missing data were addressed	Methods, Study Design and Participants (exclusions); Figure 1
12d	If applicable, describe analytical methods taking account of sampling strategy	Not applicable
12e	Describe any sensitivity analyses	Methods, Statistical Analysis (sensitivity analysis with interaction terms)
Results		
13a	Report numbers of individuals at each stage of study—eg numbers potentially eligible, examined for eligibility, confirmed eligible, included in the study, completing follow-up, and analysed	Results, paragraph 1; Figure 1
13b	Give reasons for non-participation at each stage	Figure 1
13c	Consider use of a flow diagram	Figure 1
14a	Give characteristics of study participants (eg demographic, clinical, social) and information on exposures and potential confounders	Results, paragraphs 1–2; Table 1
14b	Indicate number of participants with missing data for each variable of interest	Table 1 (N column); Figure 1
15	Report numbers of outcome events or summary measures	Results, paragraphs 2–3; Table 1 (BME prevalence)
16a	Give unadjusted estimates and, if applicable, confounder-adjusted estimates and their precision (eg, 95% confidence interval). Make clear which confounders were adjusted for and why they were included	Results; Table 2; Figure 3
16b	Report category boundaries when continuous variables were categorized	Methods, Study Design and Participants (BMI, CRP thresholds)
16c	If relevant, consider translating estimates of relative risk into absolute risk for a meaningful time period	Not applicable (cross-sectional design)
17	Report other analyses done—eg analyses of subgroups and interactions, and sensitivity analyses	Results (sex-stratified analyses); Table 2; Supplementary Table 5
Discussion		
18	Summarise key results with reference to study objectives	Discussion, paragraphs 1–2

Continued on next page

Table S10 continued from previous page

Item No	Recommendation	Reported on page/section
19	Discuss limitations of the study, taking into account sources of potential bias or imprecision. Discuss both direction and magnitude of any potential bias	Discussion, Limitations paragraph
20	Give a cautious overall interpretation of results considering objectives, limitations, multiplicity of analyses, results from similar studies, and other relevant evidence	Discussion, paragraphs 3–8
21	Discuss the generalisability (external validity) of the study results	Discussion (comparison to prior studies); Limitations
Other Information		
22	Give the source of funding and the role of the funders for the present study and, if applicable, for the original study on which the present article is based	Abstract (Funding); Role of the Funding Source

Reference: von Elm E, et al. The Strengthening the Reporting of Observational Studies in Epidemiology (STROBE) statement: guidelines for reporting observational studies. J Clin Epidemiol. 2008;61(4):344-9.

3 NAKO MRI Study Centers and Principal Investigators

Table 11: NAKO MRI Study Centers and Principal Investigators

MRI Study Center	Principal Investigator (Epidemiology)	Principal Investigator (Imaging)
Augsburg	Prof. Dr. Annette Peters, Helmholtz Munich	Prof. Dr. Thomas Kröncke, University Hospital Augsburg
Berlin-North	Prof. Dr. Tobias Pischon, Max Delbrück Center for Molecular Medicine	Prof. Dr. Thoralf Niendorf, Max Delbrück Center for Molecular Medicine
Essen	Prof. Dr. Andreas Stang, University Hospital Essen	Prof. Dr. Michael Forsting, University Hospital Essen
Mannheim	Prof. Dr. Rudolf Kaaks, German Cancer Research Center (DKFZ)	Prof. Dr. Hans-Ulrich Kauczor, University Hospital Heidelberg
Neubrandenburg	Prof. Dr. Henry Völzke, University Medicine Greifswald	Dr. Robin Bülow, University Medicine Greifswald

NAKO MRI Imaging Core:

- Prof. Dr. Fabian Bamberg, University of Freiburg (Lead)
- Prof. Dr. Christopher Schlett, University of Freiburg (Deputy)

4 References

1. Diaz-Pinto A, Alle S, Nath V, et al. MONAI Label: A Framework for AI-Assisted Interactive Labeling of 3D Medical Images. *Medical Image Analysis* 2024;95:103207.

2. Lowekamp BC, Chen DT, Ibáñez L, Blezek D. The Design of SimpleITK. *Frontiers in Neuroinformatics* 2013;7:45.

3. Cardoso MJ, Li W, Brown R, et al. MONAI: An Open-Source Framework for Deep Learning in Healthcare. 2022. Available at: http://arxiv.org/abs/2211.02701.